Anti-Breast Cancer Stem Cell Properties of Silver(I)-Non-Steroidal Anti-Inflammatory Drug Complexes

SINGH, Karampal, SINGH, Kuldip, JOHNSON, Alice and SUNTHARALINGAM, Kogularamanan

EurJIC
European Journal of Inorganic Chemistry

Research Article
doi.org/10.1002/ejic.202400133

Chemistry Europe
European Chemical Societies Publishing

www.eurjic.org

Anti-Breast Cancer Stem Cell Properties of Silver(I)-Non-Steroidal Anti-Inflammatory Drug Complexes

Karampal Singh,[a] Kuldip Singh,[a] Alice Johnson,*[a, b] and Kogularamanan Suntharalingam*[a]

The synthesis and characterisation of a series of silver(I) complexes (**1**–**7**) containing non-steroidal anti-inflammatory drugs (NSAIDs) and triphenylphosphine ligands is reported. The diclofenac-containing silver(I) complex **1** exhibits micromolar potency towards bulk breast cancer cells and breast cancer stem cells (CSCs) cultured in monolayers. Notably, the silver(I) complex **1** displays up to 9.4-fold higher potency towards three-dimensional mammospheres than cisplatin (a clinically used anticancer metallodrug) and salinomycin (a breast-CSC active small molecule). Mechanistic studies show that the silver(I) complex **1** readily interacts with thiol-containing biomolecules in solution and elevates intracellular reactive oxygen species levels in breast CSCs. Interestingly the silver(I) complex **1** does not perturb cyclooxygenase-2 (COX-2) expression in breast CSCs and its cytotoxicity is unaffected in the presence of prostaglandin E2, implicative of a COX-2 independent mechanism of action.

Introduction

Cancer is a major cause of death worldwide with nearly one in six deaths recorded in 2020 resulting from the illness.[1] One of the frontline treatment options for cancer is chemotherapeutics in the form of metal-containing small molecules.[2] Patients presenting with testicular, ovarian, cervical, colorectral, head and neck tumours are routinely treated with platinum(II)-based agents, cisplatin, carboplatin, oxaliplatin, nedaplatin, heptaplatin, and lobaplatin, and those presenting with acute promyelocytic leukaemia are commonly administered the arsenic(III)-based agent, arsenic trioxide.[2a,3] Although the current clinically-approved metallodrugs available to cancer specialists are effective against certain tumour types at certain progression stages, they have distinct drawbacks that lead to inadequate patient outcomes.[2a,4] This includes systemic toxicity arising from the inability of metallodrugs to differentiate between proliferating cancer cells and other fast growing non-cancerous cells.[5] Some cancer cells exhibit inherent or acquired resistance towards metallodrugs and thus survive treatment regimens comprising of metallodrugs.[2b,4] Cancer stem cells (CSCs) are sub-populations of tumour cells that not only evade metallodrugs (and other forms of chemotherapeutics) at their administered doses but also activate tumour (re)growth and promote metastasis.[6] The stem cell-like nature of CSCs enables them to differentiate, self-renew, and exhibit slow cell cycle profiles, all of these properties allow CSCs to survive metallodrug treatment and prompt relapse and metastasis.[7] The development of metal complexes that can remove CSCs (and other chemoresistant cancer cell sub-populations) at clinically relevant doses is a major unmet challenge in medicinal inorganic chemistry.[8] Over the last decade we and others have developed several metal complexes and determined their anti-CSC properties in *in vitro* and *in vivo* systems.[9] Unfortunately, despite these efforts, a metallodrug with the appropriate stability profile and CSC efficacy has not been identified to support progression beyond preclinical evaluation.

Silver and silver-containing compounds have been used for centuries in water sanitisation, the treatment of burn wounds, and the prevention of eye infections.[10] The application of silver complexes as antimicrobial agents has also been widely investigated,[11] however, their use as anticancer agents is relatively underexplored.[12] Strikingly, the cellular mechanism of action of most anticancer silver complexes has not been fully resolved.[12] A wide range of silver(I) complexes with nitrogen, phosphorus and sulphur donor ligands, *N*-heterocyclic carbene, carboxylic acid and amino acid groups have been developed and tested in various *in vitro* and *in vivo* cancer models.[12–13] The effectiveness of silver(I) complexes as anti-CSC agents has been very rarely studied. Thus far, only one silver(I) complex, containing dithiacyclam, has been tested in CSC systems.[14] The silver(I)-dithiacyclam complex displayed micromolar potency towards breast CSCs grown in monolayer and three-dimensional cultures.[14] Mechanistic studies revealed that the silver(I)-dithiacyclam complex reacted rapidly with thiol-containing biomolecules and subsequently elevated intracellular reactive oxygen species (ROS) levels and induced apoptotic breast CSC death.[14]

[a] *K. Singh, K. Singh, Dr. A. Johnson, Dr. K. Suntharalingam*
School of Chemistry
University of Leicester
Leicester, UK
E-mail: k.suntharalingam@leicester.ac.uk

[b] *Dr. A. Johnson*
Biomolecular Sciences Research Centre
Sheffield Hallam University
Sheffield, UK
E-mail: alice.johnson@shu.ac.uk

Supporting information for this article is available on the WWW under https://doi.org/10.1002/ejic.202400133

Research Article
doi.org/10.1002/ejic.202400133

In this study we sought to prepare silver(I) complexes containing two stabilising phosphine ligands and a panel of non-steroidal anti-inflammatory drugs (NSAID) and determine their anti-breast CSC properties. NSAIDs are inhibitors of cyclo-oxygenase-2 (COX-2),[15] an enzyme that is overexpressed in CSC-enriched breast tumours.[16] Elevated levels of COX-2 indicate poor prognosis in breast cancer patients and are correlated with advanced tumour progression and large tumor size.[17] COX-2 is also connected to breast CSC regulation stemness, and their propensity to metastasise.[18] We have previously combined copper(II), manganese(II), zinc(II), and gold(I) with various NSAIDs to prepare metal-NSAID complexes with potent and selective breast CSC activity.[19] Mono- and bi-nuclear silver(I) complexes containing NSAIDs (namely mefenamic acid, tolfenamic acid, salicylic acid, diclofenac, ibuprofen, naproxen, and nimesulide) have been reported to display micromolar potency towards bulk breast cancer cells,[20] however no silver(I) complexes containing NSAIDs have been challenged with breast CSCs. Here we investigate the anti-breast CSC activity of a series of silver(I)-NSAID complexes for the first time, and provide insight into the cytotoxic mechanism of action of the most effective complex.

Results and Discussion

Synthesis and Characterisation of Silver(I)-Non-Steroidal Anti-Inflammatory Drug Complexes

A family of silver(I) complexes **1**–**7** with various NSAID motifs and two auxiliary triphenylphosphine ligands were synthesised according to Figure 1A. Four of the silver(I)-NSAID complexes (**1**, **3**, **6**, and **7**) have been previously reported however the synthetic methods used were different to those reported by us herein.[20d–g] The corresponding NSAID (diclofenac, naproxen, ibuprofen, indomethacin, diflunisal, mefenamic acid or salicylic acid) was reacted with an equimolar amount of Ag-(acetylacetonate)$(PPh_3)_2$[21] in dichloromethane in the dark. The resultant solution was then filtered and concentrated prior to the addition of pentane to precipitate the silver(I)-NSAID complexes **1**–**7** as white or yellow solids in reasonable yields (48–91 %). The silver(I)-NSAID complexes **1**–**7** were fully characterised by ^{1}H, ^{31}P{^{1}H} (and ^{19}F{^{1}H}) NMR and infra-red spectroscopy, elemental analysis, and single crystal X-ray crystallography (Figures S1–S18, Tables S1–S3, see ESI). Preservation of the Ag-PPh_3 unit in the silver(I)-NSAID complexes **1**–**7** was evidenced by a distinctive signal (8.29 to 9.66 ppm) in their ^{31}P{^{1}H} NMR spectra at room temperature (Figures S2, S4, S6, S8, S10, S13, and S15). As expected, the ^{31}P signals associated to **1**–**7** were downfield shifted relative free triphenylphosphine, (−5.55 ppm).[19d] The ^{31}P{^{1}H} NMR spectra of **1**–**7** were also recorded at low temperature (193 K) (Figure S16). Both ^{107}Ag- and ^{109}Ag-^{31}P coupling were observed ($^{1}J_{Ag\text{-}P}$ ranging from 421–444 Hz for ^{107}Ag-^{31}P and 484–510 Hz for ^{109}Ag-^{31}P), further proving the existence of the Ag-PPh_3 unit within **1**–**7**. The variance between the vibrational stretching frequencies of the asymmetric, $\nu_{asym}(CO_2)$ and symmetric, $\nu_{sym}(CO_2)$ carboxylato peaks gives an indication of the binding mode of the associated carboxylic acid group to a given metal centre.[22] According to the IR spectra, the difference between $\nu_{asym}(CO_2)$ and $\nu_{sym}(CO_2)$ stretching bands for **1**–**7** varied between 173–193 cm^{-1} (Figure S17), suggestive of a bidentate coordination mode for the carboxylate group on the NSAIDs to the silver(I) centre. The purity of **1**–**7** in their solid form was confirmed by elemental analysis (see ESI). Single crystals of **1**–**7** suitable for X-ray diffraction studies were obtained by layer-diffusion of hexane into a dichloromethane solution of **1**–**7** (CCDC 2333721–2333727, Figures 1B, S18 and Tables S1–S2).[23] Selected bond distances and bond angles data are presented in Table S3. The structures of **1**–**7** each consists of a four-coordinate silver(I) centre with a distorted tetrahedral geometry. The silver(I) is bound to two triphenylphosphine ligands via the phosphorus atom and the corresponding NSAID motif via both oxygen atoms within the carboxylato group. The silver(I) coordination sphere is consistent with the spectroscopic and analytic data for **1**–**7** discussed previously. The average bond angles around the silver(I) centre varied from 104.63° to 105.98°, consistent with a distorted tetrahedral geometry. Further, the Ag–O and Ag–P

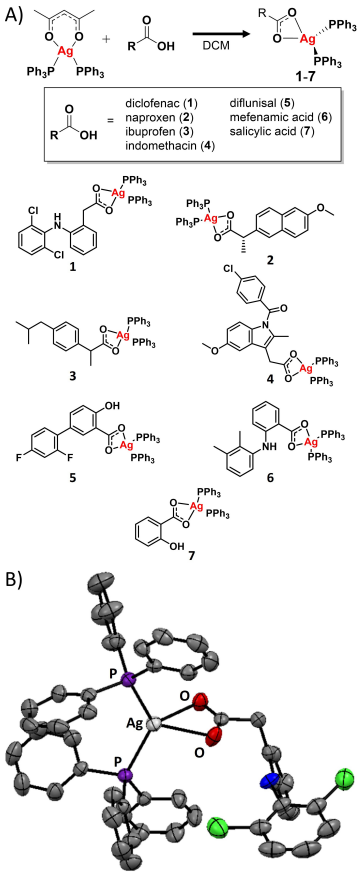

Figure 1. (A) Reaction scheme for the preparation of the silver(I) complexes containing triphenylphosphine and diclofenac, naproxen, ibuprofen, indomethacin, diflunisal, mefenamic acid or salicylic acid (**1**–**7**). (B) X-ray structure of **1** comprising of triphenylphosphine and diclofenac. Thermal ellipsoids are drawn at 50 % probability. C atoms are shown in grey, N in dark blue, O in red, P in purple, Cl in green, and Ag in silver. The H atoms have been omitted for clarity.

bond distances are consistent with related tetrahedral silver(I) complexes.[20d–g,24]

Hydrophobicity and Solution Stability

The hydrophobicity of the silver(I)-NSAID complexes **1**–**7** was determined by measuring the extent to which **1**–**7** partitioned between water and octanol using inductively coupled plasma mass spectrometry (ICP-MS). The experimentally determined LogP values varied from 1.07 ± 0.01 to 1.60 ± 0.13 (Table S4). The LogP values for **1**–**7** suggest that the complexes should be sufficiently soluble in aqueous solutions for cell-based studies and be readily internalised by dividing cells. This assertion is based on the fact that the LogP values of analogues copper(I)-NSAID complexes range from 0.82 ± 0.002 to 1.25 ± 0.06 and these complexes are readily internalised by breast CSCs (235 ± 5 to 302 ± 4 ng of Cu/ million cells upon addition of 5 μM for 24 h).[25] The stability of **1**–**7** in solution was initially gauged using UV-vis spectroscopy. In DMSO, the UV-vis absorbance trace associated to **1**–**4** (50 μM) remained largely the same over the course of 24 h at 37 °C suggestive of good solution stability (Figure S19). In contrast, the UV-vis absorbance traces associated to **5**–**7** (50 μM) changed markedly, and for **5** and **6** isosbestic point(s) were observed, suggestive of reactivity and instability in solution (Figure S19). Time course $^{31}P\{^{1}H\}$ and ^{1}H NMR spectroscopy studies were carried out to confirm the solution stability of **1**–**7**. The $^{31}P\{^{1}H\}$ NMR spectra for **1**–**3** (10 mM) in DMSO-d_6 at 37 °C displayed a single signal throughout the course of 72 h (7.60 ppm for **1**, 7.36 ppm for **2**, and 7.25 ppm for **3**) corresponding to the intact complexes (Figures S20-S22). The ^{1}H NMR spectra for **1**–**3** (10 mM) in DMSO-d_6 remained largely unaltered over the same period, under the same conditions (Figures S23–S25). The $^{31}P\{^{1}H\}$ and ^{1}H NMR spectra for **4**–**7** in DMSO-d_6 displayed distinct changes over the course of 72 h (Figures S26-S33). In the $^{31}P\{^{1}H\}$ NMR spectra, a signal corresponding to triphenylphosphine oxide (at *ca.* 25.5 ppm) appeared after 24 h or 48 h and persisted at 72 h (Figures S26–S29). It should be noted that the $^{31}P\{^{1}H\}$ signal corresponding to intact **4**–**7** was also observed after 72 h. As expected, triphenylphosphine oxide and intact **4**–**7** were detected in the ^{1}H NMR spectra (Figures S30–S33). This suggests that **4**–**7** are only partially stable in solution. Collectively, the time course UV-vis and NMR spectroscopy experiments indicate that out of the seven silver(I)-NSAID complexes prepared, only **1**–**3** are stable in solution and hence appropriate for cell-based studies.

Activity Towards Bulk Breast Cancer Cells and Breast Cancer Stem Cells

The cytotoxicity of the solution stable silver(I)-NSAID complexes **1**–**3** towards bulk breast cancer cells (HMLER) and breast CSC-enriched cells (HMLER-shEcad) grown in monolayer cultures was determined using the MTT assay. The IC_{50} values (concentration required to decrease cell viability by half) were interpolated from dose-response curves (Figures S34–S36) and are summarised in Table 1. The silver(I)-NSAID complexes **1**–**3** displayed similar potencies towards bulk breast cancer cells and breast CSC, in the micromolar range. More specifically, the silver(I)-NSAID complexes **1**–**3** were slightly more potent towards HMLER cells than HMLER-shEcad cells with the diclofenac-bearing complex **1** exhibiting the lowest toxicity differential (0.29 μM, the concentration difference between the IC_{50} values for HMLER and HMLER-shEcad cells) within the series. This implies that **1** is best suited to removing bulk breast cancer cells and breast CSCs with a single dose. The potency of the silver(I)-NSAID complexes **1**–**3** towards HMLER and HMLER-shEcad cells was similar to salinomycin and cisplatin.[19a,b] Salinomycin is a monocarboxylic polyether ionophore found to have promising anti-breast CSC properties in preclinical studies.[26] Cisplatin is a DNA-targeting, square-planar platinum(II)-based drug used in the clinic to treat various forms of cancer.[3b] The NSAID components present in **1**–**3** (diclofenac, naproxen, and ibuprofen) displayed significantly lower potency towards HMLER and HMLER-shEcad cells compared to **1**–**3** (Figure S37, Table S5), implying that the silver(I)-*bis*-triphenylphosphine motif in **1**–**3** is responsible for its potency.[19b,27] This notion was supported by the fact that Ag(acetylacetonate)$(PPh_3)_2$ displayed similar potencies towards HMLER and HMLER-shEcad cells as **1**–**3** (Figure S38, Table S5). Ag(acetylacetonate)$(PPh_3)_2$ was not investigated further *in vitro* as time course $^{31}P\{^{1}H\}$ and ^{1}H NMR spectroscopy studies in DMSO-d_6 over 72 h revealed the presence of triphenylphosphine oxide, indicative of instability in solution (Figures S39–S40).

Activity Towards Breast Cancer Stem Cell Spheroids

Breast CSCs grown in low attachment, serum-free conditions tend to clump together to form spherical structures called mammospheres.[28] Mammospheres are collections of hundreds of breast CSCs that are more representative of tumours than breast CSCs grown in two-dimensional monolayer cultures. The addition of **1**–**3** (at their IC_{20} value for 5 days) to single cell suspensions of HMLER-shEcad cells markedly reduced the

Table 1. IC_{50} values of the silver(I)-NSAID complexes **1**–**3**, cisplatin, and salinomycin against HMLER cells, HMLER-shEcad cells, and HMLER-shEcad mammospheres.

Compound	HMLER IC_{50} [μM][a]	HMLER-shEcad IC_{50} [μM][a]	Mammosphere IC_{50} [μM][b]
1	1.40 ± 0.01	1.69 ± 0.18	1.97 ± 0.01
2	1.36 ± 0.11	2.25 ± 0.06	1.98 ± 0.01
3	0.77 ± 0.03	1.97 ± 0.01	2.00 ± 0.02
cisplatin[c]	2.57 ± 0.02	5.65 ± 0.30	13.50 ± 2.34
salinomycin[c]	11.43 ± 0.42	4.23 ± 0.35	18.50 ± 1.50

[a] Determined after 72 h incubation (mean of three independent experiments ± SD). [b] Determined after 120 h incubation (mean of two independent experiments ± SD). [c] Reported in ref. [19a–b, and 29].

Research Article
doi.org/10.1002/ejic.202400133

number and size of mammospheres formed (Figures 2A–B). The inhibitory effect of **1**–**3** on mammosphere formation was comparable or better than salinomycin and cisplatin (upon dosage at their IC_{20} value for 5 days) under identical conditions (Figure 2A). The effect of **1**–**3** on mammosphere viability was determined using the colorimetric resazurin-based reagent, TOX8. The IC_{50} values (concentration required to reduce mammosphere viability by half) of **1**–**3** were in the low micromolar range (Figure S41 and Table 1). Notably, the mammosphere IC_{50} value for the diclofenac-bearing complex **1** was 9.4-fold and 6.8-fold lower than salinomycin and cisplatin, respectively.[29] Taken together, the mammosphere studies show that the silver(I)-NSAID complexes are able to inhibit mammosphere formation (both in terms of number and size) and reduce mammosphere viability.

Reaction with Thiol-Containing Biomolecules and Intracellular Redox Modulation

The cytotoxicity of several silver(I) complexes is linked to their ability to interact with thiol groups in proteins.[30] Therefore, the interaction of the diclofenac-bearing complex **1** with model thiol-containing biomolecules, *N*-acetylcysteine (NAC) and glutathione (GSH), was probed using $^{31}P\{^1H\}$ and ^1H NMR spectroscopy (over 72 h at 37 °C). $^{31}P\{^1H\}$ NMR studies in DMSO-d_6 revealed that the addition of **1** (10 mM) to a stoichiometric amount of NAC or GSH yielded $[Ag^I(NAC)(PPh_3)_n]$ or $[Ag^I(GSH)(PPh_3)_n]$ (n = 1 or 2) respectively and triphenylphosphine oxide (*ca.* 25.50 ppm) (Figures S42–S43). The formation of $[Ag^I(NAC)(PPh_3)_n]$ or $[Ag^I(GSH)(PPh_3)_n]$ was immediate whereas triphenylphosphine oxide was detected after 24 h. ^1H NMR studies corroborated the $^{31}P\{^1H\}$ NMR data, indicating the formation of $[Ag^I(NAC)(PPh_3)_n]$ or $[Ag^I(GSH)(PPh_3)_n]$ and free triphenylphosphine oxide (Figures 3 and S44). The ^1H NMR studies also indicated the possible release of diclofenac (Figures 3 and S44). For the experiment involving **1** and GSH, precipitation of a white solid was observed after 72 h. ICP-MS analysis of the precipitate indicated the presence of silver. This suggests that **1** reacts with GSH to form a poorly soluble extended silver-containing polymeric network (in addition to the products identified that stay in solution). This is consistent with the formation of extended polymeric networks upon reaction of silver(I) salts with biologically relevant thiols.[31] $[Ag^I(NAC)(PPh_3)_n]$ and $[Ag^I(GSH)(PPh_3)_n]$ (n = 1 or 2) were prepared independently *in situ* by reacting $[Ag^I(acetylacetonate)(PPh_3)_2]$[21] with NAC or GSH in DMSO-d_6, to confirm the aforementioned assignments. Overall, the NMR spectroscopy studies suggest that **1** is able to interact with thiol-containing biomolecules to form silver adducts or polymeric networks, triphenylphosphine oxide, and possibly diclofenac.

As the diclofenac-bearing complex **1** is able to readily interact with thiol-containing biomolecules, and moreover with GSH, it could perturb the GSH redox buffering system in breast CSCs and promote intracellular ROS elevation.[32] The potential for **1** to increase intracellular ROS levels in HMLER-shEcad cells was probed using 6-carboxy-2′,7′-dichlorodihydro-fluorescein diacetate (DCFH-DA), an established ROS indicator. HMLER-shEcad cells treated with **1** ($2\times IC_{50}$ value) did not display elevated intracellular ROS levels at very short exposure times (0.5–3 h), however after 6 h exposure, a substantial increase in intracellular ROS levels (79% increase, $p < 0.05$) was observed (Figure 4). The intracellular ROS levels increased further upon 16 h and 24 h exposure (3.7- to 4.3-fold compared to untreated cells) (Figure 4). Taken together, the NMR spectroscopy and ROS studies indicate that **1** has the ability to elevate intracellular ROS levels, potentially via interaction with GSH and modulation of the GSH redox buffering system.

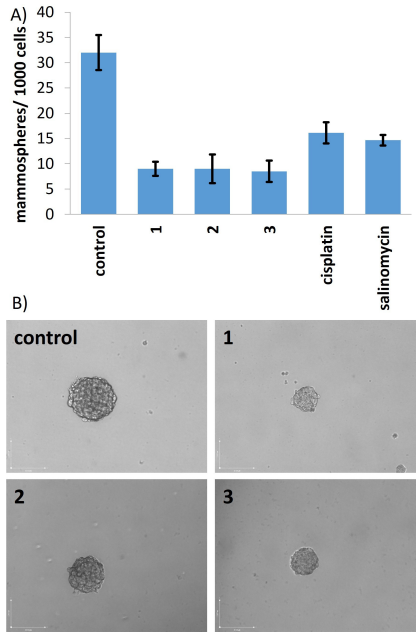

Figure 2. (A) Quantification of mammosphere formation with HMLER-shEcad cells untreated and treated with **1**, **2**, **3**, salinomycin or cisplatin (at their IC_{20} values, 5 days). Error bars represent standard deviations. (B) Representative bright-field images (×10) of HMLER-shEcad mammospheres in the absence and presence of **1**, **2** or **3** (at their IC_{20} values, 5 days).

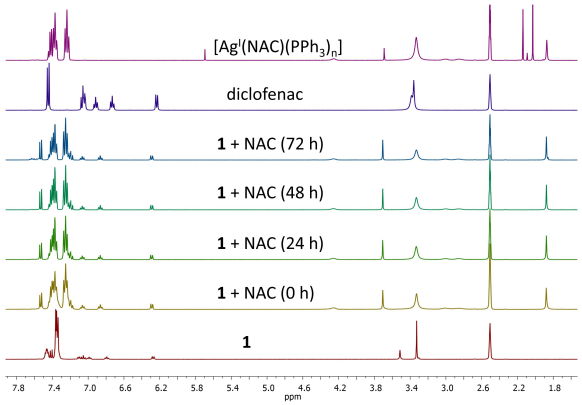

Figure 3. ^1H NMR spectra for complex **1** (10 mM) in DMSO-d_6, in the absence and presence of *N*-acetylcysteine (NAC, 10 mM) over the course of 72 h at 37 °C. The ^1H NMR spectra of diclofenac and $[Ag^I(NAC)(PPh_3)_n]$ (n = 1 or 2) (both 10 mM) in DMSO-d_6 are also provided.

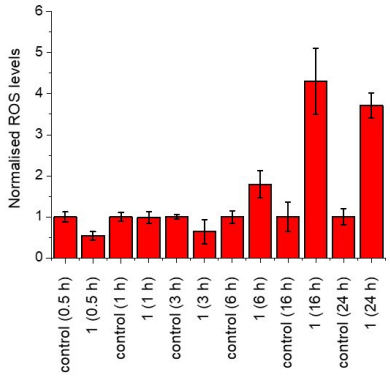

Figure 4. Normalised ROS activity in untreated HMLER-shEcad cells (control) and HMLER-shEcad cells treated with **1** (2 × IC_{50} value for 0.5, 1, 3, 6, 16, and 24 h).

Cyclooxygenase-2 Independent Mechanism of Action

As the silver(I)-NSAID complex **1** contains a diclofenac moiety (an established COX-2 inhibitor) and is potentially able to release diclofenac upon reaction with NAC and GSH, flow cytometric studies were conducted to determine if the mechanism of action of **1** involved COX-2 downregulation. HMLER-shEcad cells pre-treated with lipopolysaccharide (LPS) (2.5 μM for 24 h), to increase basal COX-2 levels, and dosed with **1** (IC_{50} value or 2×IC_{50} value for 48 h) did not display a marked change in COX-2 expression compared to untreated cells (Figure 5A). In contrast, diclofenac-treated (20 μM for 48 h) HMLER-shEcad cells have been shown to exhibit noticeably lower levels of COX-2 compared to untreated cells (Figure S45).[29a] To determine if **1** induces COX-2 dependent CSC death, cytotoxicity studies were performed with HMLER-shEcad cells in the presence and absence of prostaglandin E2 (PGE2) (20 μM, 72 h), the product of COX-2-facilitated arachidonic acid metabolism. The potency of **1** towards HMLER-shEcad cells slightly increased (rather than decreased) in the presence of PGE2 (IC_{50} value = 1.25 ± 0.03 μM, Figure 5B), suggesting that **1** evokes COX-2-independent CSC death. Collectively, the flow cytometric and cytotoxicity studies with PGE2 indicate that mechanism of action of **1** is most likely independent of COX-2.

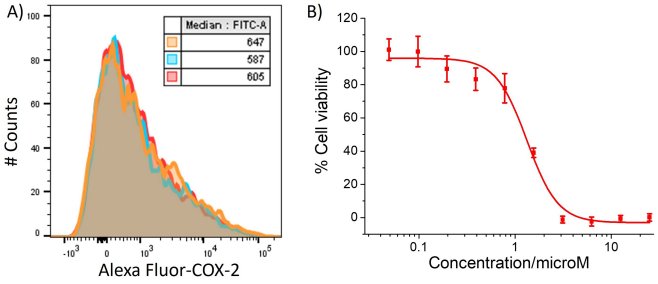

Figure 5. (A) Representative histograms displaying the green fluorescence emitted by anti-COX-2 Alexa Fluor 488 nm antibody-stained HMLER-shEcad cells treated with LPS (2.5 μM) for 24 h, followed by 48 h in media (red) or media containing **1** (IC_{50} value, blue) or **1** (2 × IC_{50} value, orange). (B) Representative dose-response curve for the co-treatment of HMLER-shEcad cells with **1** and PGE2 (20 μM) after 72 h incubation. Sigmoidal fitting parameters: χ^2: 36.48042, R^2: 0.98811, Init(A1): 95.944 (2.93), Final(A2): -3.0595 (3.62), XatY50(x0): 1.3286 (0.120), Power(p): 2.7130 (0.581).

Conclusions

In summary we report the preparation and characterisation of a family of silver(I) complexes containing NSAIDs and triphenylphosphine ligands (**1**–**7**). X-ray crystallography studies indicated that the silver(I) complexes **1**–**7** adopt tetrahedral geometries with the silver(I) atom coordinated to the corresponding NSAID moiety in a bidentate fashion and to two triphenylphosphine ligands. Out of the seven silver(I)-NSAID complexes prepared, three of the silver(I)-NSAID complexes (**1**-**3**) were deemed stable in solution according to time course UV-vis and NMR spectroscopy studies. The silver(I) complexes **1**–**3** displayed micromolar toxicity toward bulk breast cancer cells and breast CSCs grown in monolayers, similar to salinomycin and cisplatin. Strikingly, the diclofenac-containing silver(I) complex **1** exhibited 9.4- and 6.8-fold greater potency toward three-dimensional mammospheres than salinomycin and cisplatin, respectively. Cell-based mechanistic studies suggested that the diclofenac-containing silver(I) complex **1** increased intracellular ROS levels in breast CSCs. Flow cytometric and complementary cytotoxicity studies indicated that the mechanism of action of **1** is independent of COX-2. This suggests that the silver(I)-*bis*-triphenylphosphine motif is a determining factor in the mode of operation of **1**. This indication is consistent with the similar toxicities of **1** and Ag(acetylacetonate)$(PPh_3)_2$ towards breast CSCs. Overall, our results show that silver(I) complexes can be used to effectively kill breast CSCs grown in monolayers and three-dimensional cultures, and could cultivate further explorations into the anti-CSC properties of silver(I) complexes.

Experimental Section

Materials and Methods

All synthetic procedures were performed under normal atmospheric conditions. ^1H, $^{31}P\{^1H\}$ and $^{19}F\{^1H\}$ NMR were recorded at room temperature on a Bruker Avance 400 spectrometer (^1H 400.0 MHz, ^{31}P 162.0 MHz, ^{19}F 376.5 MHz) with chemical shifts (δ, ppm) reported relative to the peaks of the residual protic solvent. Fourier transform infrared (FTIR) spectra were recorded with an IRAffinity-1S Shimadzu spectrophotometer. UV-vis absorption spectra were recorded on a Cary 3500 UV-Vis spectrophotometer. Inductively coupled plasma mass spectrometry (ICP-MS) were measured using a Thermo Scientific ICAP-Qc quadrupole ICP mass spectrometer. Elemental analysis of the compounds prepared was performed commercially by the University of Cambridge. The NSAIDs (diclofenac, naproxen, ibuprofen, indomethacin, diflunisal, mefenamic acid or salicylic acid) were purchased from Sigma-Aldrich and used without further purification. Solvents were purchased from Fisher and used without further purification. [Ag(acetylacetonate)$(PPh_3)_2$] was prepared using a reported protocol.[21]

General synthesis of the silver(I)-NSAID triphenylphosphine complexes, 1–7. To a solution of the corresponding NSAID (0.1 mmol) in dichloromethane (5 mL) was added [Ag(acetylacetonate)$(PPh_3)_2$] (0.1 mmol) and the mixture stirred for 2 h

in the dark. The resultant solution was filtered through celite and concentrated to minimum volume under vacuum. Pentane (10 mL) was added to precipitate a white or yellow solid which was collected and dried under vacuum to give the corresponding Ag(I)-NSAID complexes **1**–**7**.

Ag(I)-diclofenac complex 1: white solid, 84.5 mg, 91%; ^{1}H NMR (400 MHz, DMSO-d_6) δ 9.75 (s, 1H, NH), 7.50–7.42 (m, 6H, PPh_3), 7.41 (d, J = 8.1 Hz, 2H, CH_{k+m}), 7.37–7.31 (m, 24H, PPh_3), 7.10 (dd, J = 7.4, 1.4 Hz, 1H, CH_g), 7.05 (t, J = 8.0 Hz, 1H, CH_i), 6.98 (td, J = 7.7, 1.5 Hz, 1H, CH_e), 6.78 (td, J = 7.4, 1.0 Hz, 1H, CH_f), 6.27 (d, J = 7.7 Hz, 1H, CH_d), 3.51 (s, 2H, CH_2); ^{31}P{^{1}H} NMR (162 MHz, DMSO-d_6) δ 7.60 (s, PPh_3); ATR-FTIR (solid, cm^{-1}): 395, 426, 439, 486, 500, 515, 523, 548, 593, 618, 649, 692, 706, 741, 762, 770, 781, 836, 851, 923, 935, 997, 1026, 1044, 1071, 1094, 1155, 1168, 1182, 1194, 1236, 1250, 1279, 1306, 1316, 1378 ($CO_{2\ sym}$), 1433, 1454, 1479, 1514, 1555 ($CO_{2\ asym}$), 1573, 1588, 1602, 3046; Anal. Calcd. $C_{50}H_{40}AgCl_2NO_2P_2$: C 64.74, H 4.35, N 1.51; Found: C 64.27, H 4.23, N 1.54.

Ag(I)-naproxen complex 2: white solid, 43.3 mg, 50%; ^{1}H NMR (400 MHz, DMSO-d_6) δ 7.69 −7.66 (m, 3H, $CH_e + CH_g + CH_l$), 7.52–7.29 (m, 31H, $PPh_3 + CH_m$), 7.25 (d, J = 2.5 Hz, 1H, CH_j), 7.09 (dd, J = 9.0, 2.6 Hz, 1H, CH_h), 3.86 (s, 3H, Me_n), 3.69–3.60 (m, 1H, CH_b), 1.42 (d, J = 7.1 Hz, 3H, Me_c); ^{31}P{^{1}H} NMR (162 MHz, DMSO-d_6) δ 7.34 (s, PPh_3); ATR-FTIR (solid, cm^{-1}): 400, 426, 432, 478, 500, 618, 692, 743, 811, 851, 867, 877, 888, 927, 997, 1028, 1061, 1094, 1159, 1176, 1213, 1232, 1250, 1264, 1359, 1384 ($CO_{2\ sym}$), 1433, 1458, 1479, 1505, 1557 ($CO_{2\ asym}$), 1586, 1604, 3054; Anal. Calcd. $C_{50}H_{43}AgO_3P_2 \cdot H_2O$: C 68.27, H 5.16, N 0.00; Found: C 68.13, H 4.66, N 0.00.

Ag(I)-ibuprofen complex 3: white solid, 40.5 mg, 48%; ^{1}H NMR (400 MHz, CD_2Cl_2) δ 7.44–7.24 (m, 32H, $PPh_3 + CH_f + CH_h$), 7.01 (d, J = 8.1 Hz, 2H, $CH_e + CH_i$), 3.62 (q, J = 7.1 Hz, 1H, CH_b), 2.43 (d, J = 7.1 Hz, 2H, CH_2), 1.90–1.79 (m, 1H, CH_k), 1.42 (d, J = 7.1 Hz, 3H, Me_c), 0.90 (d, J = 6.6 Hz, 6H, $Me_l + Me_m$); ^{31}P{^{1}H} NMR (162 MHz, CD_2Cl_2) δ 8.29 (s, PPh_3); ATR-FTIR (solid, cm^{-1}): 397, 424, 439, 498, 511, 620, 692, 727, 746, 799, 844, 877, 997, 1028, 1069, 1096, 1157, 1182, 1287, 1306, 1326, 1351, 1380 ($CO_{2\ sym}$), 1433, 1460, 1479, 1512, 1559, 1573 ($CO_{2\ asym}$), 1586, 2867, 2910, 2924, 2951, 2976, 3046, 3060, 3071; Anal. Calcd. $C_{49}H_{47}AgO_2P_2 \cdot 0.5H_2O$: C 69.51, H 5.71, N 0.00; Found: C 69.22, H 5.50, N 0.00.

Ag(I)-indomethacin complex 4: yellow solid, 67.4 mg, 68%; ^{1}H NMR (400 MHz, CD_2Cl_2) δ 7.54 (d, J = 8.5 Hz, 2H, $CH_n + CH_r$), 7.44–7.20 (m, 32H, $PPh_3 + CH_o + CH_q$), 7.06–7.03 (m, 2H, $CH_e + CH_h$), 6.63 (dd, J = 9.0, 2.6 Hz, 1H, CH_g), 3.64 (s, 3H, Me_s), 3.56 (s, 2H, CH_2), 2.19 (s, 3H, Me_k); ^{31}P{^{1}H} NMR (162 MHz, CD_2Cl_2) δ 8.35 (s, PPh_3); ATR-FTIR (solid, cm^{-1}): 432, 482, 500, 548, 601, 626, 647, 663, 694, 748, 799, 811, 834, 857, 916, 995, 1015, 1036, 1069, 1096, 1143, 1157, 1176, 1225, 1264, 1283, 1328, 1353, 1380 ($CO_{2\ sym}$), 1400, 1435, 1456, 1479, 1559 ($CO_{2\ asym}$), 1571, 1594, 1604, 1656, 1676, 2833, 2927, 2954, 2990, 3052, 3069; Anal. Calcd. $C_{55}H_{45}AgClNO_4P_2 \cdot 0.5H_2O$: C 66.18, H 4.64, N 1.40, Found: C 66.13, H 4.52, N 1.61.

Ag(I)-diflunisal complex 5: white solid, 44.3 mg, 50%; ^{1}H NMR (400 MHz, CD_2Cl_2) δ 8.05 (dd, J = 2.2, 1.5 Hz, 1H, CH_g), 7.58–7.20 (m, 32H, $PPh_3 + CH_e + CH_m$), 6.97–6.85 (m, 3H, $CH_d + CH_j + CH_l$); ^{31}P{^{1}H} NMR (162 MHz, CD_2Cl_2) δ 9.66 (s, PPh_3); ^{19}F{^{1}H} NMR (376 MHz, CD_2Cl_2) δ −113.93 (d, J = 7.52 Hz), -114.34 (d, J = 7.52 Hz); ATR-FTIR (solid, cm^{-1}): 391, 432, 500, 529, 599, 661, 692, 743, 816, 832, 842, 886, 904, 921, 966, 997, 1028, 1071, 1096, 1139, 1159, 1184, 1215, 1254, 1264, 1277, 1295, 1302, 1341, 1380 ($CO_{2\ sym}$), 1411, 1435, 1479, 1561 ($CO_{2\ asym}$), 1592, 1625, 3054; Anal. Calcd. $C_{49}H_{37}AgF_2O_3P_2 \cdot H_2O$: C 65.42, H 4.37, N 0.00; Found: C 65.74, H 4.15, N 0.00.

Ag(I)-mefenamic acid complex 6: white solid, 65.2 mg, 75%; ^{1}H NMR (400 MHz, CD_2Cl_2) δ 10.45 (s, 1H, NH), 8.05 (dd, J = 7.9, 1.7 Hz, 1H, CH_f), 7.52–7.23 (m, 30H, PPh_3), 7.19 (d, J = 7.9 Hz, 1H, CH_i), 7.13 (ddd, J = 8.3, 7.2, 1.7 Hz, 1H, CH_d), 7.02 (t, J = 7.7 Hz, 1H, CH_j), 6.90 (dd, J = 8.3, 1.0 Hz, 1H, CH_c), 6.85 (d, J = 7.4 Hz, 1H, CH_k), 6.64 (ddd, J = 7.9, 7.2, 1.0 Hz, 1H, CH_e) 2.28 (s, 3H, Me_o), 2.08 (s, 3H, Me_n); ^{31}P{^{1}H} NMR (162 MHz, CD_2Cl_2) δ 8.88 (s, PPh_3); ATR-FTIR (solid, cm^{-1}): 393, 414, 441, 500, 515, 573, 618, 692, 741, 785, 811, 820, 840, 914, 968, 997, 1026, 1042, 1069, 1094, 1145, 1157, 1180, 1285, 1330, 1370, 1396 ($CO_{2\ sym}$), 1433, 1448, 1479, 1489, 1542, 1578 ($CO_{2\ asym}$), 1608, 3054, 3069, 3163; Anal. Calcd. $C_{51}H_{44}AgNO_2P_2 \cdot H_2O$: C 68.77, H 5.21, N 1.57; Found: C 68.69, H 4.96, N 1.74.

Ag(I)-salicylic acid complex 7: white solid, 59.4 mg, 77%; ^{1}H NMR (400 MHz, DMSO-d_6) δ 16.00 (s, 1H, OH), 7.67 (dd, J = 7.6, 1.8 Hz, 1H, CH_g), 7.53–7.35 (m, 30H, PPh_3), 7.13 (ddd, J = 8.2, 7.2, 1.8 Hz, 1H, CH_e), 6.63–6.57 (m, 2H, $CH_d + CH_f$); ^{31}P{^{1}H} NMR (162 MHz, DMSO-d_6) δ 8.43 (s, PPh_3); ATR-FTIR (solid, cm^{-1}): 389, 432, 490, 505, 540, 618, 667, 692, 704, 741, 813, 861, 888, 912, 966, 997, 1028, 1069, 1094, 1141, 1155, 1184, 1225, 1256, 1306, 1339, 1386 ($CO_{2\ sym}$), 1409, 1433, 1458, 1481, 1565, 1573 ($CO_{2\ asym}$), 1590, 1621, 3052; Anal. Calcd. $C_{43}H_{35}AgO_3P_2$: C 67.11, H 4.58, N 0.00; Found: C 66.83, H 4.48, N 0.00.

X-ray crystallography. The crystal data for all compounds are compiled in Tables S1–S3. Crystals were mounted in inert oil on micromounts and examined using a Bruker D8 Quest diffractometer with a Photon III detector and a microfocus source with Cu–Kα radiation (λ = 1.54178) at 150(2) K. Intensities were integrated from data recorded on 1° frames by ω or φ rotation. A multi-scan method absorption correction with a beam profile was applied.[33] The structures were solved using SHELXS[34] or SHELXT;[35] the datasets were refined by full-matrix least-squares on reflections with $F^2 \geq 2\sigma(F^2)$ values, with anisotropic displacement parameters for all non-hydrogen atoms, and with constrained riding hydrogen geometries;[2] U_{iso}(H) was set at 1.2 (1.5 for methyl groups) times U_{eq} of the parent atom. The largest features in final difference syntheses were close to heavy atoms and were of no chemical significance. SHELX[34–35] was employed through OLEX2 for structure solution and refinement.[36] The CCDC deposition numbers 2333721–2333727 contain the supplementary crystallographic data. This data can be obtained free of charge via The Cambridge Crystallography Data Centre.

Measurement of water-octanol partition coefficient (LogP). The LogP value for **1**–**7** was determined using the shake-flask method and inductively coupled plasma mass spectrometry (ICP-MS). The 1-octanol used in this experiment was pre-saturated with water. A DMSO solution of **1**–**7** (10 μL, 10 mM) was incubated with 1-octanol (495 μL) and H_2O (495 μL) in a 1.5 mL tube. The tube was shaken at room temperature for 24 h. The two phases were separated by centrifugation and the content of **1**–**7** in the water phase was determined by ICP-MS (Thermo Scientific ICAP-Qc quadrupole ICP mass spectrometer).

Cell culture. The human mammary epithelial cell lines, HMLER and HMLER-shEcad were kindly donated by Prof. R. A. Weinberg (Whitehead Institute, MIT). These cells are unavailable via commercial or biobank sources however the precursor primary mammary epithelial cells (HMEC) are available commercially via ATCC. HMLER and HMLER-shEcad cells were maintained in Mammary Epithelial Cell Growth Medium (MEGM) with supplements and growth factors (BPE, hydrocortisone, hEGF, insulin, and gentamicin/amphotericin-B). The cells were grown at 310 K in a humidified atmosphere containing 5% CO_2.

Cytotoxicity studies: MTT assay. Exponentially growing cells were seeded at a density of approximately 5×10^3 cells per well in 96-well flat-bottomed microplates and allowed to attach for 24 h prior to addition of compounds. Various concentrations of the test compounds (0.0004–100 μM) were added and incubated for 72 h at 37 °C (total volume 200 μL). Stock solutions of the compounds were prepared as 10 mM DMSO solutions and diluted using cell media.

The final concentration of DMSO in each well was ≤1 %. After 72 h, 20 μL of MTT (4 mg mL^{-1} in PBS) was added to each well and the plates incubated for an additional 4 h at 37 °C. The media/MTT mixture was eliminated and DMSO (100 μL per well) was added to dissolve the formazan precipitates. The optical density was measured at 550 nm using a 96-well multiscanner autoreader. Absorbance values were normalised to (DMSO-containing) control wells and plotted as concentration of compound versus % cell viability. IC_{50} values were interpolated from the resulting dose dependent curves. The reported IC_{50} values are the average of three independent experiments (n = 18).

Tumorsphere formation and viability assay. HMLER-shEcad cells (5×10^3) were plated in ultralow-attachment 96-well plates (Corning) and incubated in MEGM supplemented with B27 (Invitrogen), 20 ng mL^{-1} EGF and 4 μg mL^{-1} heparin (Sigma) for 5 days. Studies were also conducted in the presence of **1**–**3**, cisplatin, and salinomycin (0–133 μM). Mammospheres treated with **1**–**3**, cisplatin, and salinomycin (at their respective IC_{20} values, 5 days) were counted and imaged using an inverted microscope. The viability of the mammospheres was determined by addition of a resazurin-based reagent, TOX8 (Sigma). After incubation for 16 h, the fluorescence of the solutions was read at 590 nm (λ_{ex} = 560 nm). Viable mammospheres reduce the amount of the oxidised TOX8 form (blue) and concurrently increase the amount of the fluorescent TOX8 intermediate (red), indicating the degree of mammosphere cytotoxicity caused by the test compound. Fluorescence values were normalised to DMSO-containing controls and plotted as concentration of test compound versus % mammosphere viability. IC_{50} values were interpolated from the resulting dose dependent curves. The reported IC_{50} values are the average of two independent experiments, each consisting of two replicates per concentration level (n = 4).

Intracellular ROS assay. HMLER-shEcad cells (5×10^3) were seeded in each well of a 96-well plate. After incubating the cells overnight, they were treated with **1** ($2\times IC_{50}$ value for 0.5–24 h), and incubated with 6-carboxy-2′,7′-dichlorodihydrofluorescein diacetate (20 μM) for 30 min. The intracellular ROS level was determined by measuring the fluorescence of the solutions in each well at 529 nm (λ_{ex} = 504 nm). Upon incubation of 6-carboxy-2′,7′-dichlorodihydro-fluorescein diacetate (20 μM) with **1** ($2\times IC_{50}$ value) in MEGM, there was no change in emission at 529 nm (λ_{ex} = 504 nm) compared to 6-carboxy-2′,7′-dichlorodihydro-fluorescein diacetate (20 μM) alone (Figure S46). This suggests that the enhancement in emission at 529 nm (λ_{ex} = 504 nm) observed in the intracellular ROS assay involving HMLER-shEcad cells (Figure 4) is not due to an interaction between 6-carboxy-2′,7′-dichlorodihydro-fluorescein diacetate and **1**.

COX-2 Expression Assay. HMLER-shEcad cells were seeded in 6-well plates (at a density of 5×10^5 cells/ mL) and the cells were allowed to attach overnight. The cells were treated with lipopolysaccharide (LPS) (2.5 μM for 24 h), and then treated with **1** (IC_{50} value or $2\times IC_{50}$ value) or diclofenac (20 μM) and incubated for a further 48 h. The cells were then harvested by trypsinisation, fixed with 4% paraformaldehyde (at 37 °C for 10 min), permeabilised with ice-cold methanol (for 30 min), and suspended in PBS (200 μL). The Alexa Fluor® 488 nm labelled anti-COX-2 antibody (5 μL) was then added to the cell suspension and incubated in the dark for 1 h. The cells were then washed with PBS (1 mL) and analysed using a FACSCanto II flow cytometer (BD Biosciences) (10,000 events per sample were acquired) at the University of Leicester FACS Facility. The FL1 channel was used to assess COX-2 expression. Cell populations were analysed using the FlowJo software (Tree Star).

Acknowledgements

K.S. is supported by an EPSRC New Investigator Award (EP/S005544/1) and the University of Leicester. XRD crystallography at the University of Leicester is supported by an EPSRC Core Equipment Award (EP/V034766/1). We also thank the Advanced Imaging Facility (RRID:SCR_020967) at the University of Leicester for support.

Conflict of Interests

The authors declare no conflict of interest.

Data Availability Statement

The data that support the findings of this study are available from the corresponding author upon reasonable request.

Keywords: silver · cancer stem cells · non-steroidal anti-inflammatory drugs · antitumour agents · reactive oxygen species

[1] J. Ferlay, M. Colombet, I. Soerjomataram, D. M. Parkin, M. Pineros, A. Znaor, F. Bray, *Int. J. Cancer.* **2021**.
[2] a) A. Casini, A. Vessières, S. M. Meier-Menches, *Metal-based Anticancer Agents*, RSC Publishing, **2019**; b) R. L. Lucaciu, A. C. Hangan, B. Sevastre, L. S. Oprean, *Molecules* **2022**, *27*.
[3] a) S. Alassadi, M. J. Pisani, N. J. Wheate, *Dalton Trans.* **2022**, *51*, 10835–10846; b) T. C. Johnstone, K. Suntharalingam, S. J. Lippard, *Chem. Rev.* **2016**, *116*, 3436–3486; c) K. H. Antman, *Oncologist* **2001**, *6*(2), 1–2.
[4] T. C. Johnstone, G. Y. Park, S. J. Lippard, *Anticancer Res.* **2014**, *34*, 471–476.
[5] L. Kelland, *Nat. Rev. Cancer* **2007**, *7*, 573–584.
[6] M. F. Clarke, *New Eng. J. Med.* **2019**, *380*, 2237–2245.
[7] a) L. V. Nguyen, R. Vanner, P. Dirks, C. J. Eaves, *Nat. Rev. Cancer* **2012**, *12*, 133–143; b) J. Marx, *Science* **2007**, *317*, 1029–1031; c) N. Moore, S. Lyle, *J. Oncol.* **2011**, *2011*; d) L. N. Abdullah, E. K. Chow, *Clin. Transl. Med.* **2013**, *2*, 3.
[8] J. Northcote-Smith, K. Suntharalingam, *Curr. Opin. Chem. Biol.* **2023**, *72*, 102237.
[9] a) Y. Li, B. Liu, H. Shi, Y. Wang, Q. Sun, Q. Zhang, *Dalton Trans.* **2021**, *50*, 14498–14512; b) K. Laws, K. Suntharalingam, *ChemBioChem* **2018**, *19*, 2246–2253; c) A. Johnson, J. Northcote-Smith, K. Suntharalingam, *Trends Chem.* **2021**, *3*, 47–58.
[10] a) S. K. Raju, S. K, P. S, M. M, M. K, *German J. Pharm. Biomaterials* **2022**, *1*, 06–28; b) A. Munteanu, I. P. Florescu, C. Nitescu, *J. Med. Life* **2016**, *9*, 306–315.
[11] J. S. Mohler, W. Sim, M. A. T. Blaskovich, M. A. Cooper, Z. M. Ziora, *Biotechnol. Adv.* **2018**, *36*, 1391–1411.
[12] C. N. Banti, S. K. Hadjikakou, *Metallomics* **2013**, *5*, 569–596.
[13] a) W. Liu, R. Gust, *Chem. Soc. Rev.* **2013**, *42*, 755–773; b) A. Gautier, F. Cisnetti, *Metallomics* **2012**, *4*, 23–32; c) X. Liang, S. Luan, Z. Yin, M. He, C. He, L. Yin, Y. Zou, Z. Yuan, L. Li, X. Song, C. Lv, W. Zhang, *Eur. J. Med. Chem.* **2018**, *157*, 62–80.
[14] A. Johnson, L. Iffland, K. Singh, U. P. Apfel, K. Suntharalingam, *Dalton Trans.* **2021**, *50*, 5779–5783.
[15] J. R. Vane, *Nat. New. Biol.* **1971**, *231*, 232–235.
[16] L. Y. Pang, E. A. Hurst, D. J. Argyle, *Stem Cells Int.* **2016**, *2016*, 11.
[17] A. Nassar, A. Radhakrishnan, I. A. Cabrero, G. Cotsonis, C. Cohen, *Appl. Immunohistochem. Mol. Morphol.* **2007**, *15*, 255–259.
[18] a) C. Bocca, M. Ievolella, R. Autelli, M. Motta, L. Mosso, B. Torchio, F. Bozzo, S. Cannito, C. Paternostro, S. Colombatto, M. Parola, A. Miglietta, *Expert Opin. Ther. Targets* **2014**, *18*, 121–135; b) B. Singh, J. A. Berry, A. Shoher, V. Ramakrishnan, A. Lucci, *Int. J. Oncol.* **2005**, *26*, 1393–1399;

c) B. Singh, K. R. Cook, L. Vincent, C. S. Hall, C. Martin, A. Lucci, *J. Surg. Res.* **2011**, *168*, e39–49.
[19] a) J. N. Boodram, I. J. McGregor, P. M. Bruno, P. B. Cressey, M. T. Hemann, K. Suntharalingam, *Angew. Chem. Int. Ed.* **2016**, *55*, 2845–2850; b) A. Eskandari, K. Suntharalingam, *Chem. Sci.* **2019**, *10*, 7792–7800; c) T. K. Rundstadler, A. Eskandari, S. M. Norman, K. Suntharalingam, *Molecules* **2018**, *23*; d) A. Johnson, C. Olelewe, J. H. Kim, J. Northcote-Smith, R. T. Mertens, G. Passeri, K. Singh, S. G. Awuah, K. Suntharalingam, *Chem. Sci.* **2023**, *14*, 557–565.
[20] a) A. Altay, S. Caglar, B. Caglar, Z. S. Sahin, *Inorg. Chim. Acta* **2019**, *493*, 61–71; b) D. Mahendiran, R. S. Kumar, A. K. Rahiman, *Mater. Sci. Eng. C* **2017**, *76*, 601–615; c) B. Harurluoglu, A. Altay, S. Caglar, E. Kubra Kagan Yeniceri, B. Caglar, Z. Sibel Şahin, *Polyhedron* **2021**, *202*, 115189; d) C. N. Banti, A. G. Hatzidimitriou, N. Kourkoumelis, S. K. Hadjikakou, *J. Inorg. Biochem.* **2019**, *194*, 7–18; e) C. N. Banti, C. Papatriantafyllopoulou, C. Papachristodoulou, A. G. Hatzidimitriou, S. K. Hadjikakou, *J. Med. Chem.* **2023**, *66*, 4131–4149; f) F.-J. Ma, X. Huang, X.-Y. Li, S.-L. Tang, D.-J. Li, Y.-Z. Cheng, M. Azam, L.-P. Zhang, D. Sun, *J. Inorg. Biochem.* **2024**, *250*, 112404; g) M. Poyraz, C. N. Banti, N. Kourkoumelis, V. Dokorou, M. J. Manos, M. Simčič, S. Golič-Grdadolnik, T. Mavromoustakos, A. D. Giannoulis, I. I. Verginadis, K. Charalabopoulos, S. K. Hadjikakou, *Inorg. Chim. Acta* **2011**, *375*, 114–121; h) R. E. F. de Paiva, C. Abbehausen, A. F. Gomes, F. C. Gozzo, W. R. Lustri, A. L. B. Formiga, P. P. Corbi, *Polyhedron* **2012**, *36*, 112–119; i) T. Z. Candido, R. E. F. de Paiva, M. C. Figueiredo, L. de Oliveira Coser, S. C. L. Frajácomo, C. Abbehausen, I. A. Cardinalli, W. R. Lustri, J. E. Carvalho, A. L. T. G. Ruiz, P. P. Corbi, C. S. P. Lima, *Pharmaceutica* **2022**, *14*, 462.
[21] J. Chojnacki, B. Becker, A. Konitz, M. J. Potrzebowski, W. Wojnowski, *J. Chem. Soc. Dalton Trans.* **1999**, 3063–3068.
[22] a) G. B. Deacon, R. J. Phillips, *Coord. Chem. Rev.* **1980**, *33*, 227–250; b) D. Martinez, M. Motevalli, M. Watkinson, *Dalton Trans.* **2010**, *39*, 446–455.
[23] Deposition Number(s) 2333721 (for **1**), 2333722 (for **2**), 2333723 (for **3**), 2333724 (for **4**), 2333725 (for **5**), 2333726 (for **6**), 2333727 (for **7**) contain(s) the supplementary crystallographic data for this paper. These data are provided free of charge by the joint Cambridge Crystallographic Data Centre and Fachinformationszentrum Karlsruhe Access Structures service.
[24] N. R. A. Rahazat, R. A. Haque, S. W. Ng, M. R. Razali, *J. Coord. Chem.* **2015**, *68*, 1317–1331.
[25] A. Johnson, X. Feng, K. Singh, F. Ortu, K. Suntharalingam, *Molecules* **2023**, *28*, 6401.
[26] P. B. Gupta, T. T. Onder, G. Jiang, K. Tao, C. Kuperwasser, R. A. Weinberg, E. S. Lander, *Cell* **2009**, *138*, 645–659.
[27] A. Eskandari, J. N. Boodram, P. B. Cressey, C. Lu, P. M. Bruno, M. T. Hemann, K. Suntharalingam, *Dalton Trans.* **2016**, *45*, 17867–17873.
[28] G. Dontu, W. M. Abdallah, J. M. Foley, K. W. Jackson, M. F. Clarke, M. J. Kawamura, M. S. Wicha, *Genes Dev.* **2003**, *17*, 1253–1270.
[29] a) C. Lu, K. Laws, A. Eskandari, K. Suntharalingam, *Dalton Trans.* **2017**, *46*, 12785–12789; b) A. Eskandari, A. Kundu, S. Ghosh, K. Suntharalingam, *Angew. Chem. Int. Ed.* **2019**, *58*, 12059–12064.
[30] W. K. Jung, H. C. Koo, K. W. Kim, S. Shin, S. H. Kim, Y. H. Park, *Appl. Environ. Microbiol.* **2008**, *74*, 2171–2178.
[31] B. O. Leung, F. Jalilehvand, V. Mah, M. Parvez, Q. Wu, *Inorg. Chem.* **2013**, *52*, 4593–4602.
[32] F. Q. Schafer, G. R. Buettner, *Free Radical Biol. Med.* **2001**, *30*, 1191–1212.
[33] G. M. Sheldrick, *Program for Area Detector Absorption Correction*, Institute for Inorganic Chemistry, University of Göttingen: Göttingen, Germany, **1996**.
[34] G. M. Sheldrick, *Acta Crystallogr. Sect. A* **2008**, *64*, 112–122.
[35] G. M. Sheldrick, *Acta Crystallogr. Sect. C* **2015**, *71*, 3–8.
[36] O. V. Dolomanov, L. J. Bourhis, R. J. Gildea, J. A. K. Howard, H. Puschmann, *J. Appl. Crystallogr.* **2009**, *42*, 339–341.

Manuscript received: March 8, 2024
Revised manuscript received: May 22, 2024
Accepted manuscript online: May 23, 2024
Version of record online: ■■, ■■

RESEARCH ARTICLE

The existence of cancer stem cells (CSCs) is related to metastasis and relapse. A series of four-coordinate silver(I) complexes containing non-steroidal anti-inflammatory drugs and triphenylphosphine is reported to kill breast CSCs grown in monolayers and three-dimensional cultures within the micromolar range. The silver(I) complexes interact with thiol-containing biomolecules and elevate intracellular reactive oxygen species levels in CSCs.

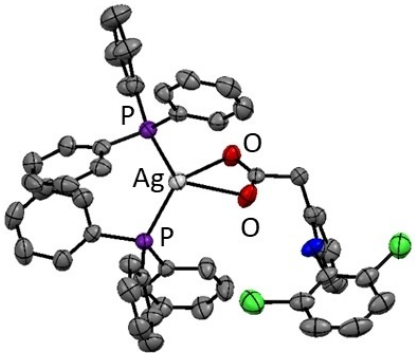

K. Singh, K. Singh, Dr. A. Johnson, Dr. K. Suntharalingam**